19th Australasian Fluid Mechanics Conference
Melbourne, Australia
8-11 December 2014

Wavelet Multiresolution Analysis on Wake Structure of a Yawed Square Cylinder

X. Lou[1], T. Zhou[1], A. Rinoshika[2] and L. Cheng[1]

[1]School of Civil, Environmental and Mining Engineering, The University of Western Australia, 35 Stirling Highway, Crawley, WA 6009, Australia

[2]Dept of Mechanical Systems Engineering, Yamagata University, Yamagata 992-8510, Japan

Abstract

The effect of yaw angle α on wake characteristics behind a yawed square cylinder was examined at a Reynolds number (Re) of 3600. Velocity and vorticity fluctuations were measured using a one-dimensional hot-wire vorticity probe. It is found that the large-scale structures contribute the most to the streamwise and transverse velocity variances, as well as Reynolds shear stress, despite the reduction as α increases. The most significant contribution to the spanwise vorticity variance comes from the small-scale structures. The independence principle (IP) for vortex shedding is also validated for $\alpha \leq 40°$.

Introduction

With increasing use of slender structures of square cross-section, the study of the wake of a square cylinder is of theoretical and practical significance. When the cylinder is yawed in a flow at an angle α (the angle between the flow direction and the plane which is perpendicular to the cylinder axis), the flow velocity in the axial direction may not be ignored and the vortex shedding characteristics may be different from a cylinder in a cross-flow. For a yawed circular cylinder, it has been found that the Strouhal number (St) and the drag coefficient, normalized by the velocity component perpendicular to the cylinder, are the same as those when the structure encounters a normal incidence flow. This is variously known as the Independence Principle (IP). Whereas the validity of IP and the flow structures of a yawed circular cylinder at different Reynolds numbers have been reported previously [8,12], our knowledge about the vortical structures of a yawed square cylinder wake is very limited [6].

A number of techniques have been developed previously to investigate the large-scale structures in turbulent wakes, such as the phase-averaged method [7], window average gradient (WAG) method [1] and the vorticity-based technique [4]. However, apart from the large-scale structures, the relatively small-scale structures, such as the secondary vortices [10], as well as the intermediate structures such as the longitudinal rib-like vortices [3], may also be of significance in the wake dynamics. Given the fact that the techniques mentioned above cannot provide details from various scales of turbulent structures, wavelet multi-resolution analysis has been introduced and proven to be effective in extracting information on the turbulent structures of the cylinder wake [3]. This method allows the measured time-frequency signals to be analysed in time-domain, frequency-domain or a combination of both. The present study aims to investigate the validity of IP for different cylinder yaw angles as well as the features of different scales of turbulence. By examining the power spectra, velocity and vorticity variances at different wavelet levels for different yaw angles, the features of the large-, intermediate- and small-scale turbulent structures in the square cylinder wake can be quantified.

Experiment details

Sketches of the one-dimensional hot-wire vorticity probe are given in figure 1. It consists of two parallel wires straddled by an X-wire. The two parallel wires are used to measure the streamwise velocity u at two locations separated by a distance Δy (=1.5 mm) and the X-wire is used to measure the streamwise velocity u and transverse velocity v (or w after a 90° rotation). The separation Δz between the two inclined wires in the X-wire is 1.6 mm. With these measured velocity components, the spanwise vorticity ω_z (or ω_y after a 90° rotation) can be calculated. This probe has been used satisfactorily to measure the spanwise and transverse vorticity components in a wake flow [2]. Measurements were conducted at a constant free stream velocity (U_∞) of 4.27 m/s and at x/d = 10 (x is the distance downstream of the cylinder and d =12.7 mm is the side length of the cylinder). The corresponding Reynolds number (Re) was about 3600. Wollaston (Pt-10% Rh) wires of 5 μm in diameter and about 1 mm in working length were operated within a constant-temperature circuit at an over heat ratio of 1.5. Signals from the circuits were offset, amplified and then digitized using a 16bit A/D converter at a sampling frequency of 10400 Hz. The sampling duration was 30 s.

Due to the imperfect spatial resolution of the probe in measuring the velocity derivatives, using the method proposed by [2], the spatial resolution of the vorticity probe in measuring the rms values for vorticity components can be corrected if local isotropy is assumed. It has been checked that when α increases from 0° to 45°, the spatial resolution of the probe improves as the Kolmogorov length scale η on the wake centreline increases from 0.11 mm to 0.13 mm. The Kolmogorov length scale is defined as $\eta = (\nu^3/<\epsilon>)^{1/4}$, where $<\epsilon>$ is the mean energy dissipation rate which can be estimated using Taylor's hypothesis. It is estimated that the root-mean-square values of the spanwise and transverse vorticity components have been underestimated by about 28%~22% for α = 0° to 45°. Unfortunately, correction for spatial resolution cannot be performed in the present study due to the lack of local isotropy at x/d = 10.

The wavelet analysis technique includes two parts, namely, the wavelet transform and the wavelet multi-resolution analysis. The former decomposes the signal into different wavelet levels to provide a useful depiction of the signal in both time and frequency, and the latter uses the discrete wavelet transform and its inverse transform to convert a signal into the sum of a number of wavelet components at different levels. One-dimensional discrete wavelet transform is a linear and orthogonal transform. Details of the wavelet method can be found in [7,10].

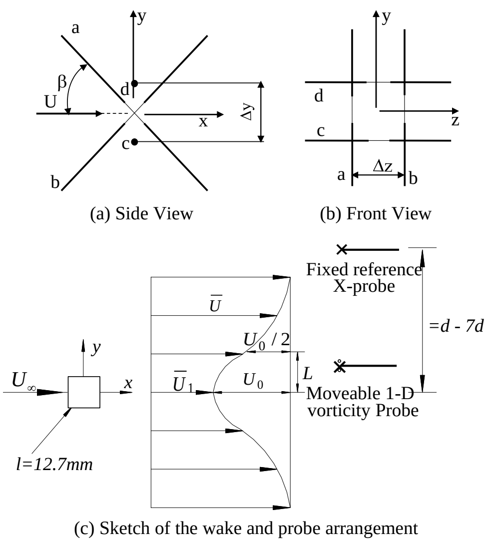

Figure 1. Sketches of the spanwise vorticity probe and probe arrangement

Results and discussion

In order to conduct wavelet analysis, a fundamental central frequency should be determined. Spectra of transverse velocity v at y/d = 0.5 are used for this purpose. The transverse velocity component was chosen here because it is more sensitive to the organized structures than the streamwise velocity or spanwise vorticity component. It is found from the spectra (figure is not shown here) that there is a strong peak on each spectrum at all yaw angles, which corresponds to the occurrence of the large-scale Kármán vortex structures. It has been checked that the three-dimensional effect has been enhanced as reflected by the increase in the spanwise velocity $\overline{W}$ when cylinder yaw angle increases (results are not shown here). This effect will cause the dispersion of vortex shedding intensity. As a result, the peak on the energy spectra becomes lower and wider as α increases. The shedding frequencies f_0 determined by the location of the peak are 44.0 Hz, 43.5 Hz, 41.4 Hz and 36.1 Hz for α = 0°, 15°, 30° and 45°, respectively. These shedding frequencies f_0, representing the organized large-scale structures, will therefore be used as the basic frequencies in the wavelet analysis. After normalisation by the velocity component normal to the cylinder axis, as implied by the IP, a Strouhal number St_N ($\equiv f_0 D/U_N$, where U_N is the velocity component normal to the cylinder axis) of are 0.131, 0.134, 0.142 and 0.152 for α = 0°, 15°, 30° and 45°, respectively, can be obtained. The above result represents a 16% deviation from the IP at α = 45°, indicating that IP will not be applicable at this yaw angle.

The velocity and vorticity signals are decomposed into 19 orthonormal wavelet levels. The higher wavelet levels correspond to lower frequency bands or large-scale structures while lower wavelet levels correspond to higher frequency bands or small-scale structures. Only results for wavelet levels 1~9 will be shown here due to the negligible contributions from levels higher than 9. Specifically, wavelet levels i = 1~3 represent the small scale-structures; i = 4~6 represent the intermediate-scale structures; i = 7 represents the organized large-scale structures located at the vortex shedding frequency band; and i = 8 and 9 represent the large-scale structures [9]. The spectra of v at wavelet levels 1–9 for α = 0° ~ 45° at y/d = 0.5 are shown in figure 2. The spectrum of each wavelet component shows a pronounced peak and spreads over a range of frequencies. The central frequency at each wavelet level can be identified from the most pronounced peak of each spectrum. These central frequencies, together with the frequency bandwidths for all wavelet levels are listed in table 1. Once the dominant frequency f_0 is set, other central frequencies at different wavelet levels are found to be about a multiple of f_0. Generally the central frequency at the i-th level is about half of that at (i-1) level due to the characteristics of wavelet basis applied in the present study.

α	0°	15°	30°	45°	Frequency bandwidth
Level 1	3040	3005	2880	2860	5200~1600
Level 2	1450	1430	1450	1398	3700~780
Level 3	760	743	701	712	1800~380
Level 4	380	370	348	353	930~190
Level 5	190	192	192	187	460~90
Level 6	88	88	86	88	230~46
Level 7	44.1	43.7	41.5	36.3	114~26
Level 8	36	31	26	24	56~13
Level 9	18	16	13	12	30~6

Table 1. Central frequency (Hz) and respective frequency bandwidth (Hz) for levels 1~9 at the wake centreline for different yaw angles.

The velocity and vorticity variances of the wavelet components $\langle \beta_i^2 \rangle$ are used to investigate the contributions of each wavelet level to velocity and vorticity variances. The wavelet variances are calculated with

$$\langle \beta_i^2 \rangle = \frac{1}{k}\sum_{i=1}^{k} \beta_i^2 \qquad (1)$$

where k is the total number of measured data points. Since the wavelet components at a central frequency lower than $0.35f_0$ (wavelet levels higher than 9) are not physically important, only the distributions for wavelet levels 1~9 at different yaw angles are shown in the present study.

For velocity variances $\langle u_i^2 \rangle$ in figure 3, the distributions at all wavelet levels are symmetrical about the wake centerline (y/d = 0). At α = 0°, the component at wavelet level 7, corresponding to the organized large-scale structures, makes the most contributions to $\langle u_i^2 \rangle$ (24%) at the peak point, followed by that at levels 8 (23%) and 6 (14%). Structures at these three levels contain the most energy. This result agrees well with that for a circular cylinder wake where the large-scale structures at $0.5f_0$ and f_0 together make the largest contribution (43%) to the Reynolds normal stresses [11]. The distributions at levels 7 (f_0) and 8 ($0.75f_0$) show double peaks at y/d = ±1.0. The contributions from both organized large-scale structures decrease significantly from 47% to 31% with the increase of the yaw angle from 0° to 45°. Though the magnitude of the contributions from the intermediate-scale structures (levels 4~6) as well as the small-scale structures (levels 1~3) keeps constant for all angles, the contribution ratio of the large-scale structures actually increases considering the decrease of the measured time-averaged value $\langle u_i^2 \rangle$, indicating the reduction of the large-scale structures at large yaw angles.

The distributions of $\langle v_i^2 \rangle$ is also symmetric about y/d = 0. In agreement with the spectra shown in figure 2a, the contribution from level 7 (organized large structures) dominates (56%) among all the wavelet levels in figure 3 at α = 0°. This is in agreement with that reported by Li and Zhou [5], who showed that $\langle v_i^2 \rangle$ (58%) at the central frequency f_0 (wavelet level 7 in the present study) overwhelmed $\langle u_i^2 \rangle$ (38%) for the rectangular cylinder wake. At the central frequency of 0.75f_0, the contribution from the large-scale structures (44%) becomes significance when α increases to 45°. This result is in agreement with that from a circular cylinder wake by Razali et al. [9], who concluded that at α = 45° the component of transverse velocity at 0.5f_0 has stronger fluctuations due to the vortex dislocation and hence increases the energy of the turbulence in the wake. Similar to the spectral features, the contribution at level 8 (37%) is comparable to that of level 7 (39%) at α = 30°. However, when α increases to 45°, the contribution at level 8 (42%) becomes dominant. Though the components at central frequencies of f_0 and 0.75f_0 (levels 7 and 8) are still the most energy containing structures, the contributions from both wavelet levels decrease from 80% to 62% as α increases from 0° to 45°. According to Rinoshika and Zhou [11], the difference in the contributions at lower central frequency (0.5f_0) highlights the difference in the turbulent structures of different wakes, which is related to the generation of large-scale coherent structures in vortex shedding. In the present study, the difference in the wake turbulence at different yaw angles can be signified by the difference in the contribution from structures at level 8 (0.75f_0), i.e. the large-scale coherent structures become relatively weak as the yaw angle increases.

The distributions of $\langle u_i v_i \rangle$ demonstrate anti-symmetric behaviour about y/d = 0 regardless of some discrepancies due to experiment uncertainty. Basically the large-scale structures at levels 7~9 dominate the contributions to $\langle u_i v_i \rangle$, in agreement with the results on the circular cylinder wake [8] that the large-scale turbulent structures at 0.5f_0 and f_0 make the largest contribution to the Reynolds stresses. Precisely, the contribution at level 7 is 54% at y/d = –1, which is the highest among all the levels at α = 0°. As α increases, this contribution decreases to 36%, 29% and 11% for 15°, 30° and 45°, respectively. The contributions from levels 8 and 9, however, increase with the yaw angle. Especially for α = 45°, the contributions from these two levels are even beyond that from level 7. When the central frequency increases from f_0 to 2f_0, a significant drop to about 3% in the contribution is observed for all yaw angles, except a slight increase in the contribution from structures of 2f_0 at α = 45°. Apart from these, the contributions from other levels to $\langle u_i v_i \rangle$ are practically negligible.

Unlike velocity components, the dominant contribution to $\langle \omega_{z,i}^2 \rangle$ comes from the small-scale structures (level 3) and followed by the intermediate-sale structures (levels 4 and 5), demonstrating that the vorticity mainly resides in the relatively small-scale structures [12]. From the investigation on a circular cylinder wake, Rinoshika and Zhou [11] found that $\langle \omega_{z,i}^2 \rangle$ corresponding to f_0 makes the smallest contribution (10%) among the frequencies concerned at the centreline of the wake. This contribution is about 16% at 2f_0 and continues to increase as the central frequency increases, reaching the maximum about 24% at 8f_0. Taking a look at the position y/d = 0 for α = 0°, the present results agree well with the above study that the contributions are about 11% at f_0 and 2f_0, about 15% at 4f_0, about 22% at 8f_0 and reaches the maximum 26% at 16f_0 regardless of the different definitions of wavelet levels at different central frequencies. As mentioned in the previous section, the component from level 7 at f_0 represents the organized coherent structures. The contribution decreases to 11%, 9%, 9% and 5% for α = 0°, 15°, 30° and 45°, respectively, suggesting a significant reduction of vortex shedding energy behind the cylinder at large yaw angles.

Conclusions

The present study suggests that IP in a square cylinder wake is applicable for α < 45°. The contributions from the organized large-scale structures dominate the variations of Reynolds stresses, followed by that from the large-scale structures (0.75f_0 and the intermediate-scale structures (2f_0). As α increases to 45°, the contribution from large-scale structures decreases significantly, indicating the dissipation of coherent structures at large yaw angles. For spanwise vorticity variation, the most significant contributions come from the small-scale structures (16f_0), which manifest the importance of incoherent structures in the form of spanwise vorticity.

Acknowledgments

The authors acknowledge the financial support from ARC through the project DP110105171.

References

[1] Antonia, R.A. & Fulachier, L., Topology of a Turbulent Boundary Layer with and without Wall Suction, *J. Fluid Mech.*, **198**, 1989, 429-451.

[2] Antonia, R.A., Zhu, Y., Shafi, H.S., Lateral vorticity measurements in a turbulent wake. J. of Fluid Mech., **323**, 1996, 173-200.

[3] Dobre, A. & Hangan, H., Investigation of the Three-dimensional Intermediate Wake Topology for a Square Cylinder at High Reynolds Number, *Expts in Fluids*, **37**, 2004, 518-530.

[4] Hussain, A.K.M.F. & Hayakawa, M., Education of Large-scale Organized Structures in a Turbulent Plane Wake, *J. Fluid Mech.*, **180**, 1987, 193-229.

[5] Li, H. & Zhou, Y., Comparison Between Triangular Cylinder and Screen Near-wakes in the Orthogonal Wavelet Rerepesentation, *JSME International Journal*, **46**, 2003, 366-376.

[6] Lou, X., Zhou, T., Zhou, Y., Wang, H. & Cheng, L., Experimental Investigation on Wake Characteristics behind a Yawed Square Cylinder, *J. of Fluids and Structures*, 2014 (submitted).

[7] Matsumura, M & Antonia, R.A., Momentum and Heat Transport in the Turbulent Intermediate Wake of a Circular Cylinder, *J Fluid Mech*., **250**, 651-668.

[8] Ramberg, S.E., The Effect of Yaw and Finite Length upon the Vortex Wakes of Stationary and Vibrating Circular Cylinders, *J. Fluid Mech.*, **128**, 1983, 81-107.

[9] Razali, S.F.M., Zhou, T., Rinoshika, A. & Cheng, L., Wavelet analysis of the turbulent wake generated by an inclined circular cylinder, *J. of Turbulence*, **11**, 2010, 1-25.

[10] Rinoshika, A. & Zhou, Y., Orthogonal Wavelet Multi-resolution Analysis of a Turbulent Cylinder Wake, *J. of Fluid Mech.*, **524**, 2005, 229-248.

[11] Rinoshika, A. & Zhou, Y., Reynolds Number Effects on Wavelet Components of Self-preserving Turbulent Structures, *Phys. Review E*, **79**, 2009, No 046322, 1-11.

[12] Zhou, T., Wang, H., Razali, S.F.M., Zhou, Y. & Cheng, L., Three-Dimensional Vorticity Measurements in the Wake of a Yawed Circular Cylinder, *Physics of Fluids*, **22**, 2010, No 015108, 1-15.

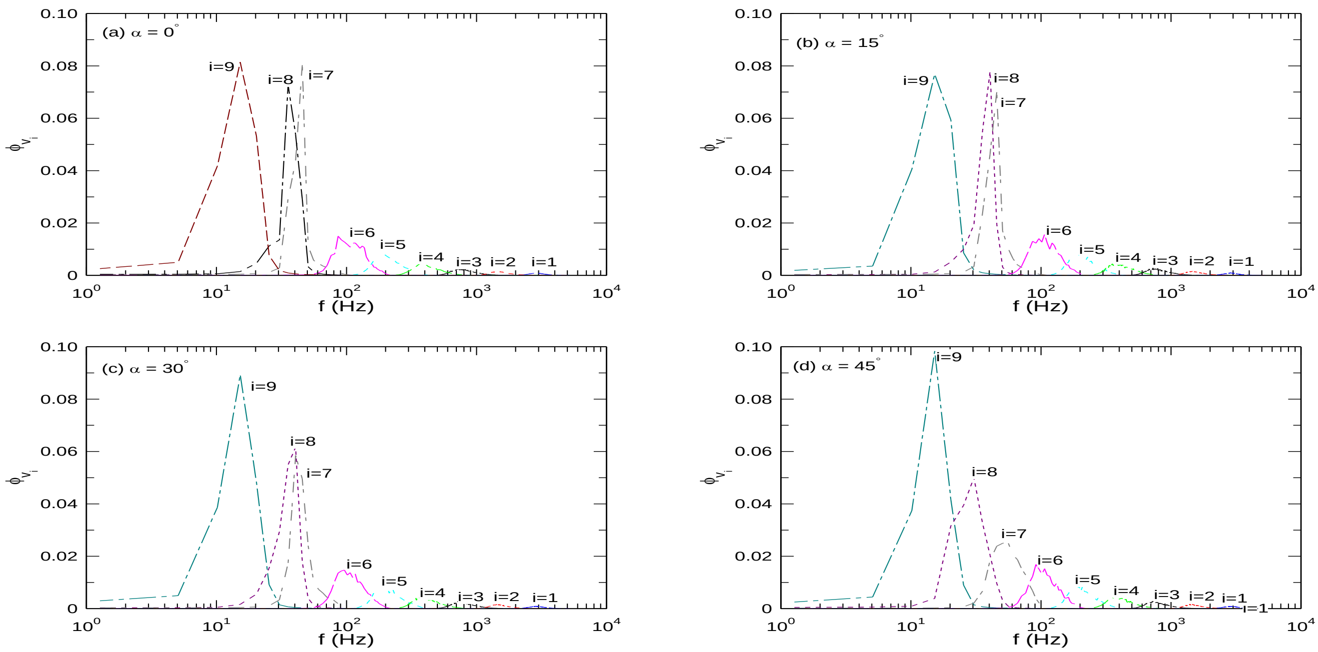

Figure 2. Comparison of energy spectra of the v-signals measured on the wake centreline and that calculated at various wavelet levels for different inclination angles.

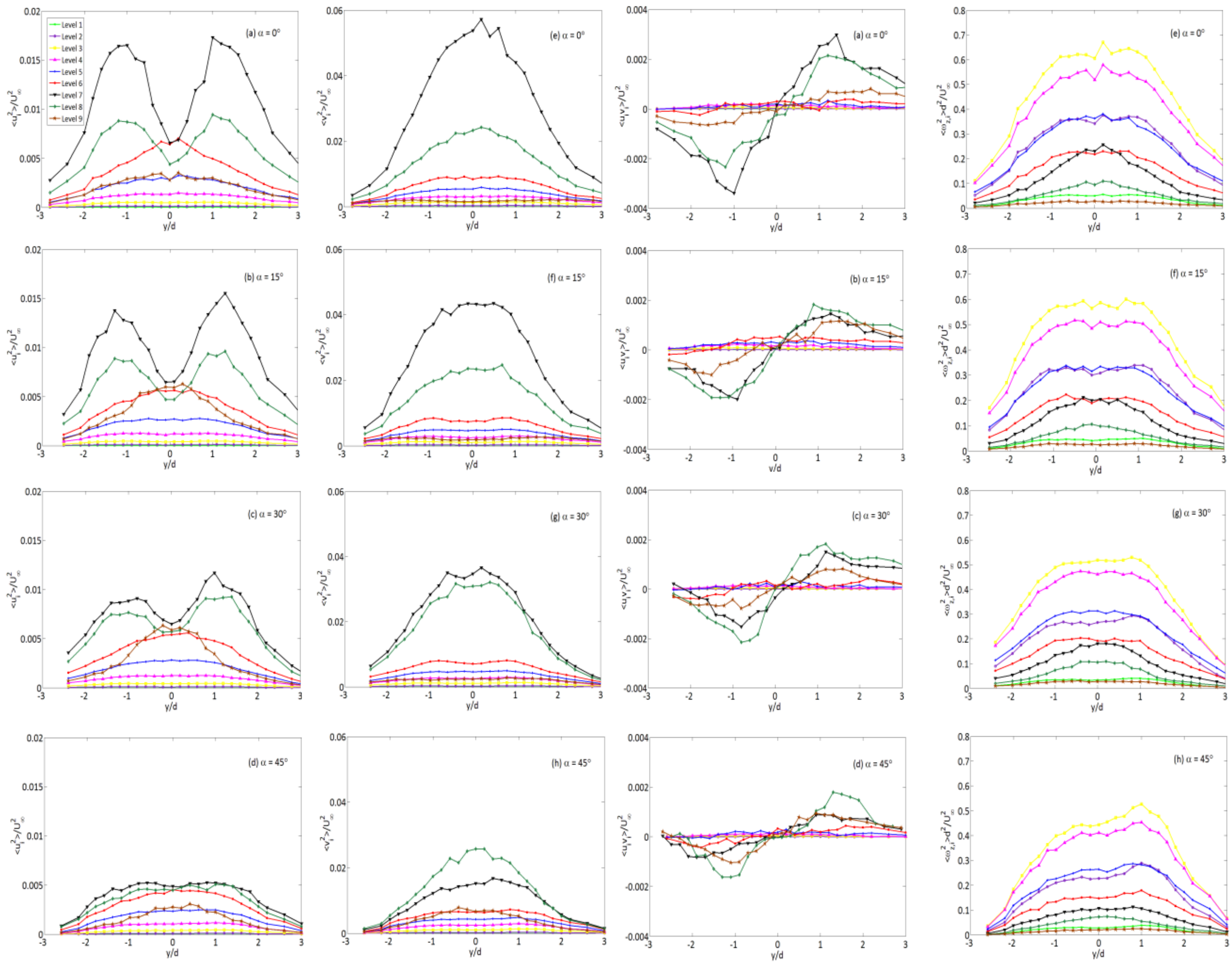

Figure 3. Variances of u, v uv and ω_z at various wavelet levels for different inclination angles.